Dictyostelium huntingtin controls chemotaxis and cytokinesis through the regulation of myosin II phosphorylation

Yu Wang[a], Paul A. Steimle[b], Yixin Ren[a], Christopher A. Ross[c], Douglas N. Robinson[a], Thomas T. Egelhoff[d], Hiromi Sesaki[a], and Miho Iijima[a]

[a]Department of Cell Biology, Johns Hopkins University School of Medicine, Baltimore, MD 21205; [b]Department of Biology, University of North Carolina at Greensboro, Greensboro, NC 27402; [c]Division of Neurobiology, Departments of Psychiatry, Pharmacology, and Neuroscience, Johns Hopkins University School of Medicine, Baltimore, MD 21205; [d]Department of Cell Biology, The Lerner Research Institute, Cleveland Clinic Foundation, Cleveland, OH 44195

ABSTRACT Abnormalities in the huntingtin protein (Htt) are associated with Huntington's disease. Despite its importance, the function of Htt is largely unknown. We show that Htt is required for normal chemotaxis and cytokinesis in *Dictyostelium discoideum*. Cells lacking Htt showed slower migration toward the chemoattractant cAMP and contained lower levels of cortical myosin II, which is likely due to defects in dephosphorylation of myosin II mediated by protein phosphatase 2A (PP2A). *htt*⁻ cells also failed to maintain myosin II in the cortex of the cleavage furrow, generating unseparated daughter cells connected through a thin cytoplasmic bridge. Furthermore, similar to *Dictyostelium htt*⁻ cells, siRNA-mediated knockdown of human HTT also decreased the PP2A activity in HeLa cells. Our data indicate that Htt regulates the phosphorylation status of myosin II during chemotaxis and cytokinesis through PP2A.

Monitoring Editor
Carole A. Parent
National Institutes of Health

Received: Nov 30, 2010
Revised: Apr 27, 2011
Accepted: May 5, 2011

INTRODUCTION

Huntingtin (Htt) is a large, evolutionarily conserved protein with a polyglutamine stretch and multiple Huntington, Elongation Factor 3, the scaffold subunit A of protein phosphatase 2A (PP2A), TOR (HEAT)-repeats. Huntington's disease, a progressive neurodegenerative disorder, is caused by expansion of the polyglutamine stretch in Htt (Ross, 2002; Harjes and Wanker, 2003; MacDonald *et al.*, 2003; Ross, 2004; Gil and Rego, 2008; Caviston and Holzbaur, 2009). In addition, it has been suggested that the loss of Htt function contributes to the pathogenesis of Huntington's disease (Harjes and Wanker, 2003; Caviston and Holzbaur, 2009). Htt is present primarily in the cytosol, and a fraction of Htt associates with organelles such as membrane vesicles, nuclei, and microtubules (Harjes and Wanker, 2003; Caviston and Holzbaur, 2009). Previous studies have also shown that Htt functions as a scaffolding protein in different cellular processes, such as intracellular signaling, membrane trafficking, apoptosis, and transcription (Harjes and Wanker, 2003; Caviston and Holzbaur, 2009). However, the exact function of Htt remains largely unknown. In this report, to determine the cellular function of Htt, we deleted the Htt gene in *Dictyostelium discoideum*, a social amoeba that has been used to study problems relevant to many human diseases (Williams *et al.*, 2006; Annesley and Fisher, 2009). We found that the *Dictyostelium* homologue of Htt is required for cytokinesis and chemotaxis through regulation of the actin-based motor protein myosin II.

In *Dictyostelium* and mammalian cells, both cytokinesis and chemotaxis share much underlying molecular architecture and many mechanisms, as they require myosin II for reorganization and accumulation at the equator of a dividing cell or at the rear of a chemotaxing cell, respectively (Robinson and Spudich, 2004; Vicente-Manzanares *et al.*, 2009; Pollard, 2010). During cytokinesis, myosin II assembles into bipolar thick filaments, accumulates in the cleavage furrow, and forms a contractile meshwork with the actin cytoskeleton to help drive cytokinesis (Uyeda and Nagasaki, 2004; Reichl *et al.*, 2008). During chemotaxis, myosin II also assembles into filaments, and then becomes concentrated in the lateral and trailing cortices of chemotaxing cells. Myosin II is involved in the posterior contraction

This article was published online ahead of print in MBoC in Press (http://www.molbiolcell.org/cgi/doi/10.1091/mbc.E10-11-0926) on May 11, 2011.

Address correspondence to: Miho Iijima (miijima@jhmi.edu).

Abbreviations used: BSA, bovine serum albumin; DB, development buffer; DTT, dithiothreitol; FBS, fetal bovine serum; GFP, green fluorescent protein; GLC, grape-like cluster; HEAT, Huntington, Elongation Factor 3, the scaffold subunit A of PP2A, TOR; Htt, huntingtin protein; MHCK, myosin heavy-chain kinase; PI3K, PI3-kinase; PP2A, protein phosphatase 2A; RFP, red fluorescent protein.

of cells, suppression of lateral pseudopodia, and disassembly of the actin network (Yumura and Uyeda, 2003; Bosgraaf and van Haastert, 2006); recent evidence also points toward myosin II inhibiting leading edge signaling (Lee *et al.*, 2010).

The localization of myosin II is regulated by at least two mechanisms in *Dictyostelium*. First, the ability of myosin II to form bipolar thick filaments is controlled by heavy-chain phosphorylation by myosin heavy-chain kinases (MHCKs); this phosphorylation drives the disassembly of the myosin bipolar thick filaments (De la Roche *et al.*, 2002; Bosgraaf and van Haastert, 2006). There are at least three MHCKs (A, B, and C) that have partially overlapping functions in myosin II phosphorylation and regulate its assembly and localization (Yumura *et al.*, 2005). In contrast, PP2A dephosphorylates myosin II, promoting its assembly. The second step in localization is recruitment of myosin II bipolar thick filaments to the cortex, which is thought to require Gbpc and Rap1 (Bosgraaf and Van Haastert, 2002; Jeon *et al.*, 2007). Myosin II localization changes in response to the chemoattractant cAMP (Yumura and Fukui, 1985; Levi *et al.*, 2002), a process that must be highly regulated. We found that the localization of myosin II was altered in *htt*⁻ cells: myosin II failed to accumulate in the cortex of cAMP-stimulated cells or in the cleavage furrow cortex during cytokinesis due to a reduction in the activity of PP2A. Our findings suggest that Htt regulates myosin II phosphorylation/dephosphorylation during chemotaxis and cytokinesis.

RESULTS

htt⁻ cells are defective in normal development and chemotaxis

Like human Htt, *Dictyostelium* Htt (DDB0238473) has a polyglutamine stretch and HEAT repeats (Supplemental Figure S1). To investigate the function of Htt, we disrupted the *Htt* gene by homologous recombination in *Dictyostelium* cells (Figure S1A) and found that Htt is important for normal development in *Dictyostelium*. When starved, *Dictyostelium* cells spontaneously aggregate and differentiate to form fruiting bodies. *htt*⁻ cells were delayed in aggregation compared with wild-type cells (Figure 1A), although the morphology and density of fruiting bodies were similar in wild-type and *htt*⁻ cells (Figure S2). Furthermore, individual *htt*⁻ cells formed small plaques on bacterial lawns (Figure 1, B and C). Exogenous expression of Htt fused to green fluorescent protein (GFP) showed even distribution in the cytoplasm of *Dictyostelium* (Figure S3, B and C), similar to human Htt (Gil and Rego, 2008), and restored normal growth in *htt*⁻ cells (Figure 1, B and C).

Because aggregation depends on chemotaxis toward cAMP during development (Swaney *et al.*, 2010), we asked whether Htt was required for chemotaxis. In this assay, we developed *htt*⁻ cells for 5 and 7 h and compared their chemotaxis to wild-type cells developed for 5 h. The longer time period for *htt*⁻ was necessary, as the expression of developmentally regulated genes, such as the cAMP receptor cAR1 and adenylate cyclase, is delayed in *htt*⁻ cells (Figure 2A). Wild-type cells developed for 5 h and *htt*⁻ cells developed for 7 h had similar amounts of cAR1 and adenylate cyclase (Figure 2A). Consistent with these observations, the *htt*⁻ cells developed for 7 h polarized normally (Figure 2, B and F) and displayed normal motility speed (Figure 2C); however, these cells showed decreases in chemotaxis speed (Figure 2D) and in chemotaxis index, which indicates the accuracy of chemotaxis (Figure 2E). These results indicate that Htt is required for normal chemotaxis.

$PtdInsP_3$ is one of the signaling molecules that regulates actin polymerization during chemotaxis (Parent *et al.*, 1998; Iijima and Devreotes, 2002) and is transiently generated in the plasma membrane upon cAMP stimulation. Production of $PtdInsP_3$ is mediated by recruitment of PI3-kinase (PI3K), which phosphorylates $PtdIns(4,5)P_2$ at the plasma membrane (Funamoto *et al.*, 2002; Iijima and Devreotes, 2002; Iijima *et al.*, 2004). We observed the production of $PtdInsP_3$ in living cells by expressing GFP fused to the PH domain of CRAC, which specifically binds to $PtdInsP_3$. GFP-PHcrac was recruited to the plasma membrane with similar kinetics in wild-type and *htt*⁻ cells when stimulated with cAMP, suggesting that $PtdInsP_3$ was produced normally in *htt*⁻ cells (Figure S4A). Likewise, PI3K-GFP translocated to the plasma membrane similarly in wild-type and *htt*⁻ cells (Figure S4B). These results suggested that $PtdInsP_3$ signaling is normal in *htt*⁻cells.

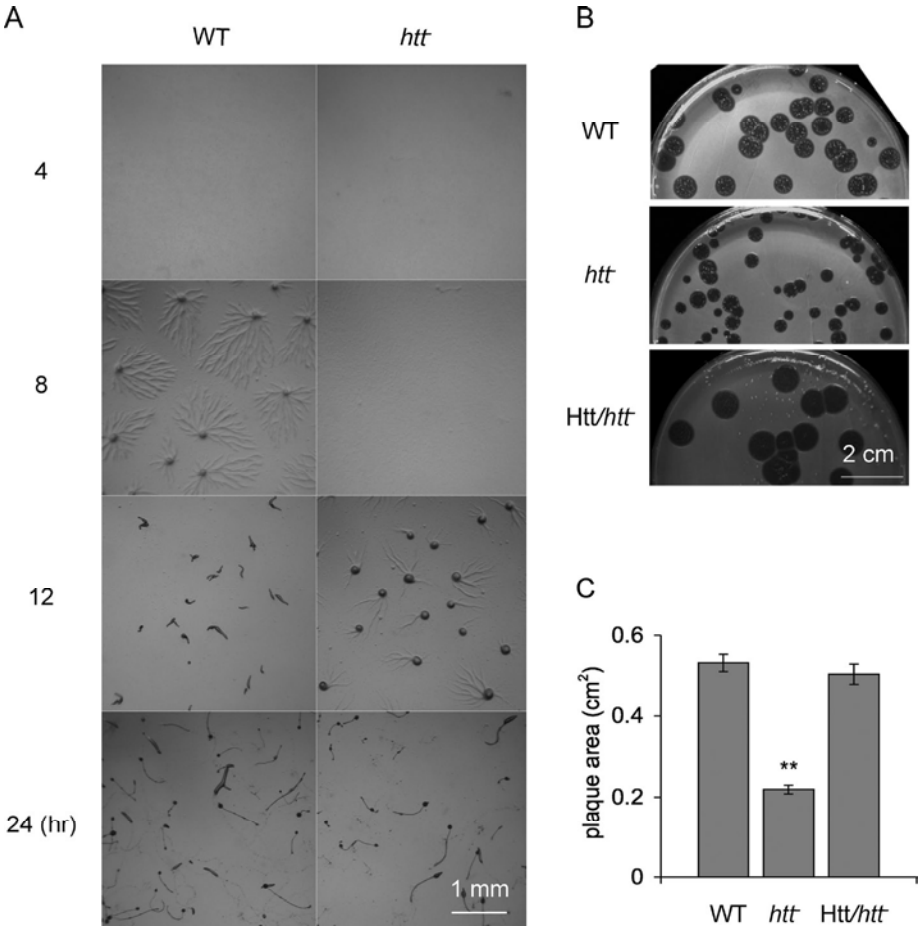

FIGURE 1: Htt is required for development in *D. discoideum*. (A) *htt*⁻ cells are delayed in development. Wild-type cells and *htt*⁻ cells were plated on nonnutrient agar at 5×10^6 cells/cm^2 to induce development. Images were taken at the indicated time points. (B) *htt*⁻ cells formed smaller plaques on the bacterial lawn. Introducing a plasmid carrying Htt-GFP in *htt*⁻ cells nearly restored the wild-type phenotype (Htt/*htt*⁻). (C) Quantification of plaque sizes. Values are mean ± SEM (n = 20).

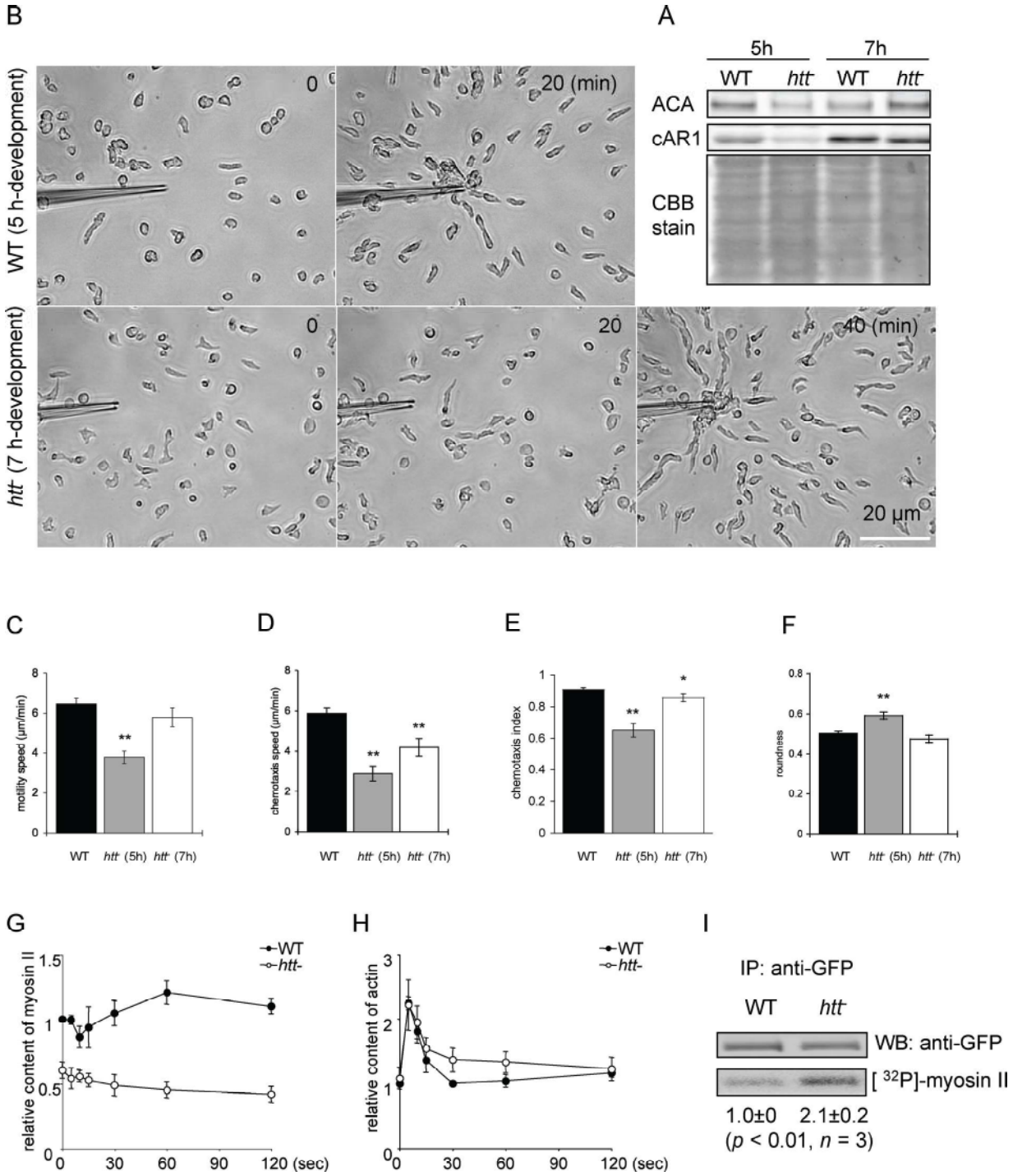

FIGURE 2: Htt is required for normal chemotaxis toward cAMP and the cortical localization of myosin II. (A) Immunoblot of the cAMP receptor, cAR1, and adenylate cyclase A (ACA) in wild-type and *htt*⁻ cells differentiated for 5 and 7 h. The protein-transferred membrane was stained with Coomassie Brilliant Blue (CBB stain) and shown as loading control. (B) Chemotaxis to a micropipette filled with 1 μM cAMP. The movements of developed wild-type (5 h) and *htt*⁻ (7 h) cells were recorded. Images were taken at the indicated time points. (C) Motility speed was determined by measuring the position of the centroid every 30 s for a period of 10 min. Results were statistically analyzed using Student's *t* test (*, $p < 0.05$; **, $p < 0.01$) in (C)–(F). (D) Chemotaxis speed was calculated as the distance toward the micropipette divided by the elapsed time (10 min). (E) Chemotaxis index was defined as the distance moved in the direction of the gradient divided by the total distance moved for 30-s intervals during a period of 10 min. (F) Roundness was determined by calculating the ratio of short axis (A_s) and long axis (A_l) of cells (A_s/A_l). Values are mean ± SEM (n = 40). Amounts of myosin II (G) and actin (H) in the Triton X-100–insoluble fraction of wild-type and *htt*⁻ cells in response to 10 μM cAMP. Values are mean ± SEM (n = 3). (I) Wild-type and *htt*⁻ cells carrying GFP-myosin II, which is expressed on top of native myosin II, were metabolically labeled with [^{32}P]orthophosphate. Whole-cell lysates were subjected to immunoprecipitation using anti-GFP antibodies, and then analyzed by immunoblotting using anti-GFP antibodies and autoradiography. Band intensity was quantified relative to wild-type levels. Values are mean ± SEM (n = 3).

A

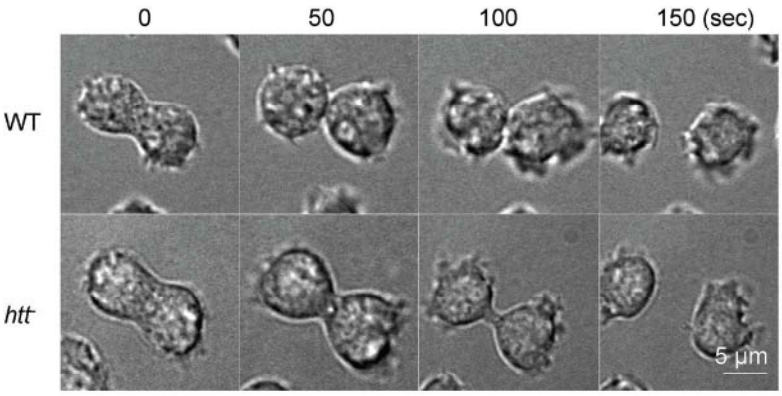

B

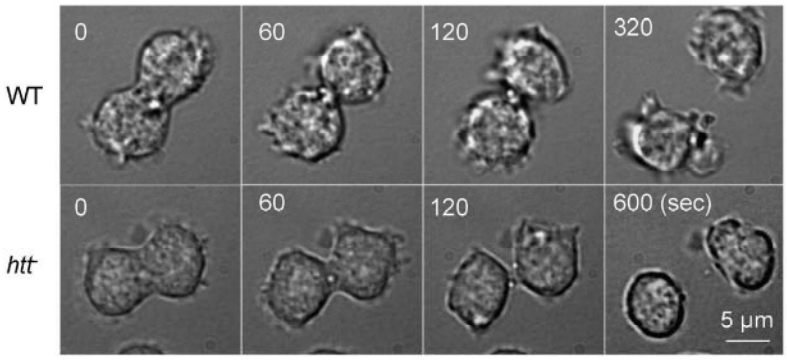

C

Substrate	Strain	Cytokinesis completion (%)	Failure (%)		n
			Fused back	Bridged	
Un-coated	WT	100	0	0	16
	htt⁻	100	0	0	17
Silicon-coated	WT	86.7	13.3	0	15
	htt⁻	66.7	0	33.3	18

D

Substrate	Strain	0-3min (%)	3-6min (%)	6-10min (%)	Average time (min)
Un-coated	WT	81.3	18.7	0	2.46±0.17
	htt⁻	76.5	23.5	0	2.21±0.18
Silicon-coated	WT	7.7	76.9	15.4	4.85±0.32
	htt⁻	0	33.3	66.7	6.64±0.55

E

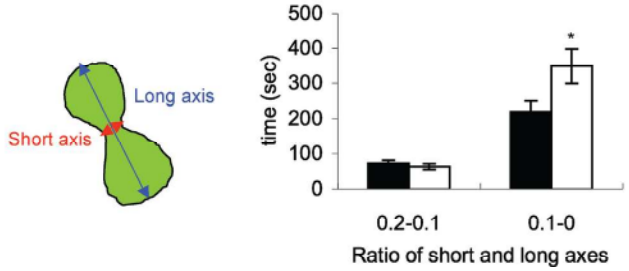

FIGURE 3: *htt*⁻ cells are defective in cytokinesis. Time-lapse images of wild-type and *htt*⁻ cells undergoing cytokinesis on coverglass (A) and on silicon-coated coverglass (B). Cells that initiated cytokinesis were identified by a short-to-long axis ratio of 0.2. The red and blue arrows represent short and long axes, respectively (E). (C) The percentages of cells that completed cytokinesis, failed to complete cytokinesis within 10 min, and fused back (Fused back) or remained dumbbell-shaped (Bridged) are shown. (D) The percentage of cells that showed the completion of cytokinesis in 0–3, 3–6, and 6–10 min. Cells that divided within 10 min were analyzed. (E) The duration of the first subphase (when the axial ratio decreased from 0.2 to 0.1) and the second subphase (when the axial ratio decreased from 0.1 to zero). Cells that divided within 10 min were analyzed.

Myosin II in the cell cortex is decreased in *htt*⁻ cells

To determine whether Htt is required for myosin II assembly and localization, we determined the amount of myosin II in the Triton X-100–insoluble cytoskeletal fraction, which represents levels of assembled myosin II in the cortex (Steimle *et al.*, 2001b). Consistent with previous observations, the amount of myosin II transiently decreased in the Triton X-100–insoluble fraction after cAMP stimulation in wild-type cells (Figure 2G). In contrast, *htt*⁻ cells showed levels of myosin II in this fraction to be ~50% of the control and showed no changes after cAMP stimulation (Figure 2G), although the total amount of myosin II was not affected. As a control, the amount of actin in the same fraction, which represents the amount of filamentous cortical actin, was transiently increased by ~2.5-fold in both wild-type and *htt*⁻ cells (Figure 2H). Therefore reduced myosin II levels were not simply due to reduced amounts of filamentous actin. We then metabolically labeled wild-type and *htt*⁻ cells expressing GFP-myosin II using [^{32}P]orthophosphate and performed immunoprecipitation using anti-GFP antibodies. Phosphorylation levels of myosin II were significantly increased by 2.1-fold in *htt*⁻ cells (Figure 2I). Thus *htt*⁻ cells have more phosphorylated myosin II, either due to enhanced kinase or reduced phosphatase activity.

htt⁻ cells are defective at later stages of cytokinesis

Myosin II is required for cytokinesis when *Dictyostelium* cells are grown on a nonadhesive substrate or in suspension culture (Robinson, 2001; Uyeda and Nagasaki, 2004). We examined the time course of cytokinesis on adhesive coverglass and less-adhesive silicon-coated coverglass. We identified cells in telophase based on cell morphology with the short-to-long axis ratio of 0.2 (Robinson and Spudich, 2004; Uyeda and Nagasaki, 2004). Wild-type and *htt*⁻ cells both completed cytokinesis similarly on the uncoated coverglass (Figure 3, A, C, and D). In contrast, on the silicon-coated substrate, almost three times as many *htt*⁻ cells as wild-type cells failed to complete cytokinesis (Figure 3, B and C). Interestingly, wild-type cells that failed to complete cytokinesis regressed the cleavage furrow, while *htt*⁻ cells that were unable to finish cytokinesis remained dumbbell-shaped and none regressed the cleavage furrow (Figure 3C). Of those cells that completed cytokinesis on silicon-coated coverglass, *htt*⁻ cells took longer to divide than wild-type cells (Figure 3D) due to a 40%

longer second phase, when the axial ratio decreased from 0.1 to zero (Figure 3E). Thus *htt*⁻ cells appeared to stall cytokinesis just before completion.

htt⁻ cells form grape-like clusters in suspension culture

Consistent with the cytokinesis defects on nonadhesive substrates, *htt*⁻ cells were severely defective in cell growth in shaken suspension cultures (Figure 4A), but not on adhesive substrates (Figure 4B). In suspension culture, *htt*⁻ cells formed clusters of cells that we named grape-like clusters (GLCs; Figure 4, C and D). Exogenous expression of *Htt* fused to GFP restored normal growth to *htt*⁻ cells, demonstrating that GLC formation results from a lack of Htt (Figure 4A). When GLCs were placed on coverglass, *htt*⁻ cells migrated away from each other and cytoplasmic connections between *htt*⁻ cells were clearly observed (Figure 4E). The intercellular connections were stretched and eventually ruptured. Furthermore, when we expressed GFP or red fluorescent protein (RFP) in the cytoplasm of *htt*⁻ cells and cultured them in shaking cultures for 3 d, individual GLCs contained only GFP or RFP (Figure 4F). These results suggest that *htt*⁻ cells remained attached through the cytoplasmic connection in GLCs. The maintenance of GLCs appears to be independent of the rearrangement of the actin cytoskeleton, as GLCs were maintained when treated for 1 h with 5 μM latrunculin A, which blocks actin polymerization (unpublished data).

htt⁻ cells fail to maintain myosin II in the cleavage furrow

To analyze the localization of myosin II, we expressed GFP-myosin II in cells and examined the ratio of GFP signals between the cleavage furrow and polar cytoplasm in dividing cells. We identified cells in telophase based on cell morphology with the short-to-long axis ratio of 0.2 and observed them until cytokinesis was completed (Robinson and Spudich, 2004; Uyeda and Nagasaki, 2004). In wild-type cells, GFP-myosin II showed ~80% stronger intensity at the cleavage furrow until the completion of cytokinesis compared with the polar cytoplasm (Figure 5, A and B), consistent with previous reports (Nagasaki *et al.*, 2002; Robinson *et al.*, 2002). In contrast, although myosin II initially accumulated in the cleavage furrow in cells with the short-to-long axis ratio of 0.2, it was gradually lost as cytokinesis progressed, and the short-to-long axis ratio became 0.1 and zero in *htt*⁻ cells (Figure 5, A and B). These data indicate that Htt helps maintain myosin II at the cleavage furrow cortex in late stages of cytokinesis.

Dephosphorylation of myosin II stimulates assembly and recruits myosin II filaments to the cortex (Murphy and Egelhoff, 1999; Yumura *et al.*, 2005; Bosgraaf and van Haastert, 2006). To test whether dephosphorylated myosin II can be maintained at the cleavage furrow in *htt*⁻ cells, we expressed a mutant form of myosin II in which three phosphorylation sites were substituted with alanine. We found that mutant myosin II continued to accumulate at the cleavage furrow in both wild-type and *htt*⁻ cells (Figure 5, C and D). Our data also suggest that dephosphorylated, assembled myosin II can be recruited to the cortex in *htt*⁻ cells.

The loss of myosin II is epistatic to the loss of Htt

If Htt is required for completion of cytokinesis through myosin II, loss of myosin II would be epistatic to Htt loss. Indeed, hpRNA-mediated knockdown of myosin II generated multinucleated giant cells in wild-type and *htt*⁻ cells (Figure 5, F and G). Therefore myosin II is required during the early stages of contractility in order to form the GLCs, and Htt is only required for maintenance of myosin II at the cleavage furrow cortex during the late stages of cytokinesis completion.

Interestingly, overexpression of MHCK-C led to the formation of large multinucleated cells in *htt*⁻ cells, but not in wild-type cells, whereas overexpression of MHCK-A resulted in multinucleated cells in both wild-type and *htt*⁻ cells (Figures 5F, S5, and S6). These results suggest that the loss of Htt renders cells more sensitive to excess phosphorylation of myosin II by MHCK-C.

The activity of PP2A is reduced in *htt*⁻ cells

To understand the mechanism underlying the altered phosphorylation status of myosin II in *htt*⁻ cells, we examined the amount (Figure 6A), localization (Figure 6B), cAMP-stimulated membrane recruitment (Figure S7), activity (Figure 6C), and autophosphorylation (Figure S8) of MHCKs. We found that MHCKs were not affected in *htt*⁻ cells. In contrast, the activity of PP2A was significantly reduced in *htt*⁻ cells (Figure 7B), while its amount and localization were not altered (Figure 7, A and C).

To test whether Htt also facilitates the activity of PP2A in human cells, we knocked down the expression of HTT using siRNA in HeLa cells (Figure 7D). As with *Dictyostelium htt*⁻ cells, knockdown of HTT resulted in a reduction in PP2A activity without affecting total amounts of PP2A (Figure 7, D and E). We also examined whether overexpression of HTT affected PP2A activity in HeLa cells and found that overexpression of either wild-type (HTT-Q17) or mutant (HTT-Q138) Htt (Rubinsztein and Carmichael, 2003) had no effect on the phosphatase activity (Figure 7, F and G). We speculate that levels of endogenous Htt are already near saturation for the regulation of PP2A activity, therefore increasing wild-type Htt levels may not change the phosphatase activity. Concerning mutant Htt overexpression, we initially thought this could show a dominant negative effect; however, the data suggest mutant Htt does not interfere with endogenous Htt function in PP2A regulation.

DISCUSSION

Our study demonstrates that Htt is required for cytokinesis and chemotaxis through the regulation of myosin II phosphorylation/dephosphorylation. As cytokinesis proceeds, *htt*⁻ cells gradually lose myosin II from the cortex of the cleavage furrow and fail to complete cell division, producing unseparated daughter cells connected by a thin cytoplasmic bridge. Similarly, myosin II levels in the cortex are reduced during chemotaxis in *htt*⁻ cells, leading to decreased migration speed. Recruitment of myosin II to the cortex requires dephosphorylation of myosin II by the phosphatase PP2A. *htt*⁻ cells displayed a reduction in PP2A activity and contained increased amounts of phosphorylated myosin II. Furthermore, our data also indicate that Htt is required for assembly of myosin II, but not for translocation to the cortex, as a phosphorylation-defective myosin II can be maintained in the cleavage furrow of *htt*⁻ cells.

PP2A consists of three subunits: catalytic, scaffolding, and regulatory. The scaffolding subunit contains the HEAT domain, which binds to the catalytic subunit. Because Htt contains HEAT domains, it is tempting to speculate that Htt may directly bind to the catalytic subunit through this domain and function as a scaffold protein, modulating the phosphatase activity or its specificity toward myosin II. In addition, Htt may regulate the assembly of PP2A. Although we found no evidence of a physical interaction between Htt and PP2A in coimmunoprecipitation studies (Y. Wang and M. Iijima, unpublished observations), it remains possible that Htt weakly and/or transiently interacts with PP2A to regulate its enzymatic activity, specificity, or assembly. Moreover, the *Dictyostelium* genome contains at least six PP2A regulatory subunits (Table S1), suggesting that PP2A likely has many functions and many

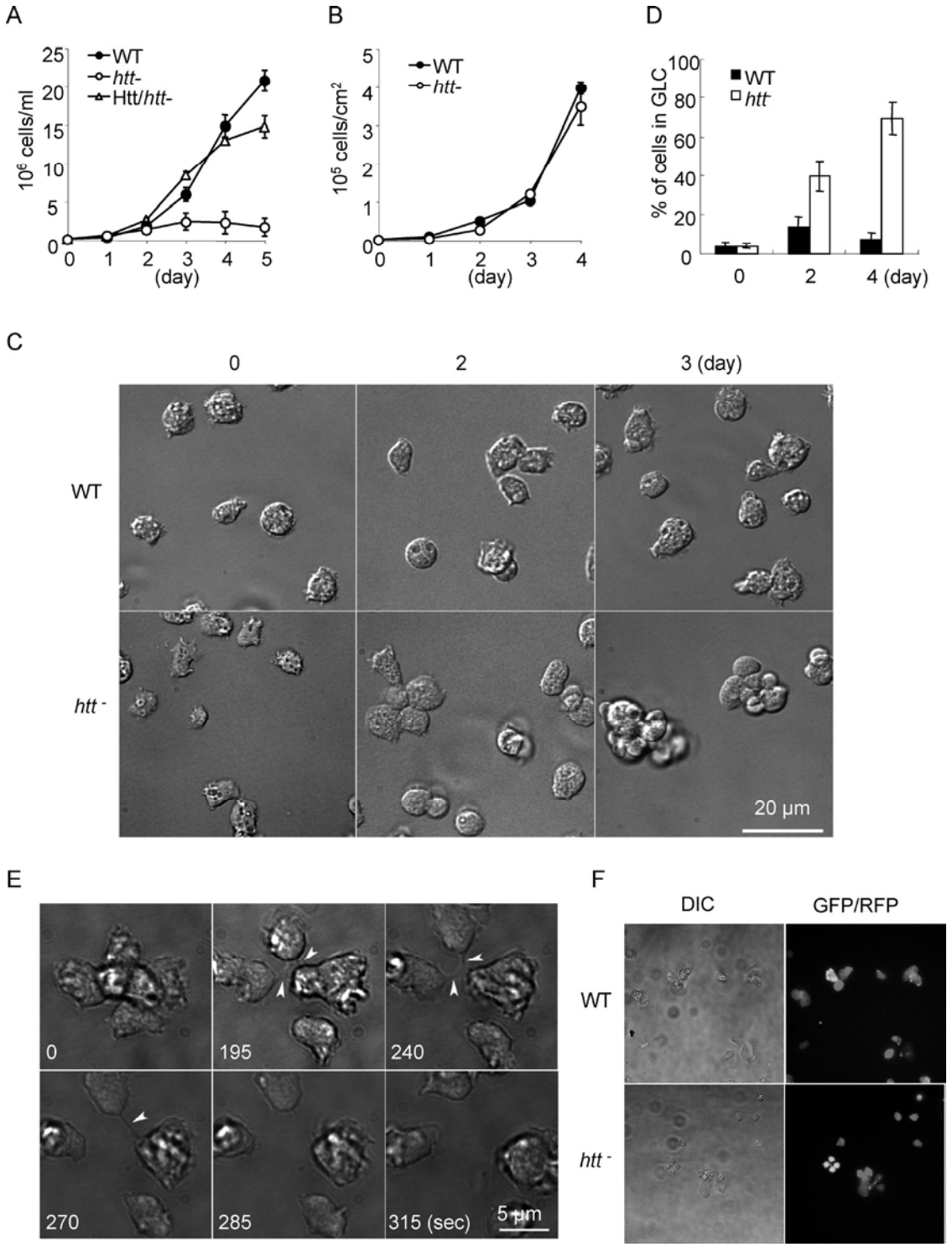

FIGURE 4: *htt*⁻ cells form grape-like clusters (GLCs) in suspension culture. Cell proliferation of wild-type cells, *htt*⁻ cells, and *htt*⁻ cells expressing GFP-*Htt* cells in suspension culture (A) and substrate-attached culture (B). Values are mean ± SEM (n = 4). (C) Formation of GLCs in shaking culture. DIC images were taken on the indicated days after transfer from substrate-attached culture to shaking culture. (D) Quantification of the number of cells in GLCs. Values are mean ± SEM (n ≥ 4). A total of 200–300 cells were scored in each experiment. (E) A GLC was placed on a glass substrate and observed by time-lapse microscopy at the indicated time points. (F) Cells expressing GFP or RFP in the cytosol were grown separately in substrate-attached culture and then mixed at the same cell density in shaking culture for 3 d. Cells were viewed by fluorescence microscopy.

substrates in *Dictyostelium* in addition to myosin II. A recent study showed that a PP2A regulatory subunit, phr2aBα, is required for myosin II assembly (Rai and Egelhoff, 2011). It would be interesting to test whether and how interactions of catalytic subunits with different regulatory subunits modulate the target specificity, phosphatase activity, and localization.

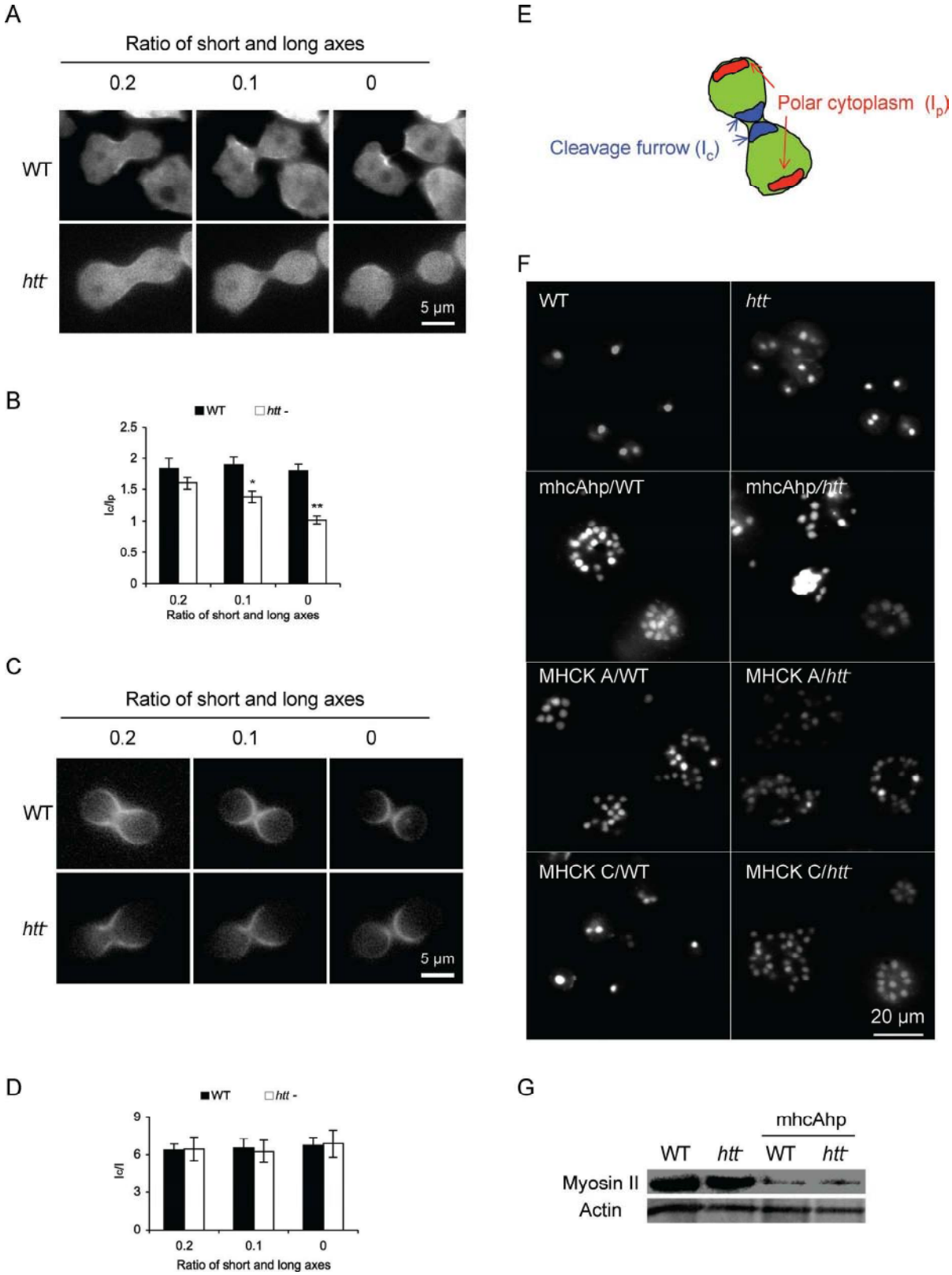

FIGURE 5: Htt is required for myosin II localization during cytokinesis. Wild-type and *htt*⁻ cells expressing GFP fused to wild-type (A) and mutant (C) myosin II were observed during cytokinesis using time-lapse fluorescence microscopy; in (C), three phosphorylation sites (Thr_{1823}, Thr_{1833}, and Thr_{2029}) are mutated. (B and D) Quantification of GFP-myosin II localization. The fluorescence intensity of the cleavage furrow (I_c) and polar cytoplasm (I_p) was measured, and the ratio of I_c/I_p is presented (E). (F) Myosin II is required for the formation of GLCs in *htt*⁻ cells. Wild-type and *htt*⁻ cells were subjected to shRNA-mediated knockdown of myosin II and grown in shaking culture for 3 d (mhcAhp/WT and mhcAhp/*htt*⁻). Wild-type and *htt*⁻ cells were transfected with MHCK-A and -C. Cells were stained with DAPI to visualize the nuclei. (G) Immunoblotting of whole-cell lysates using antibodies for myosin II heavy chain and actin.

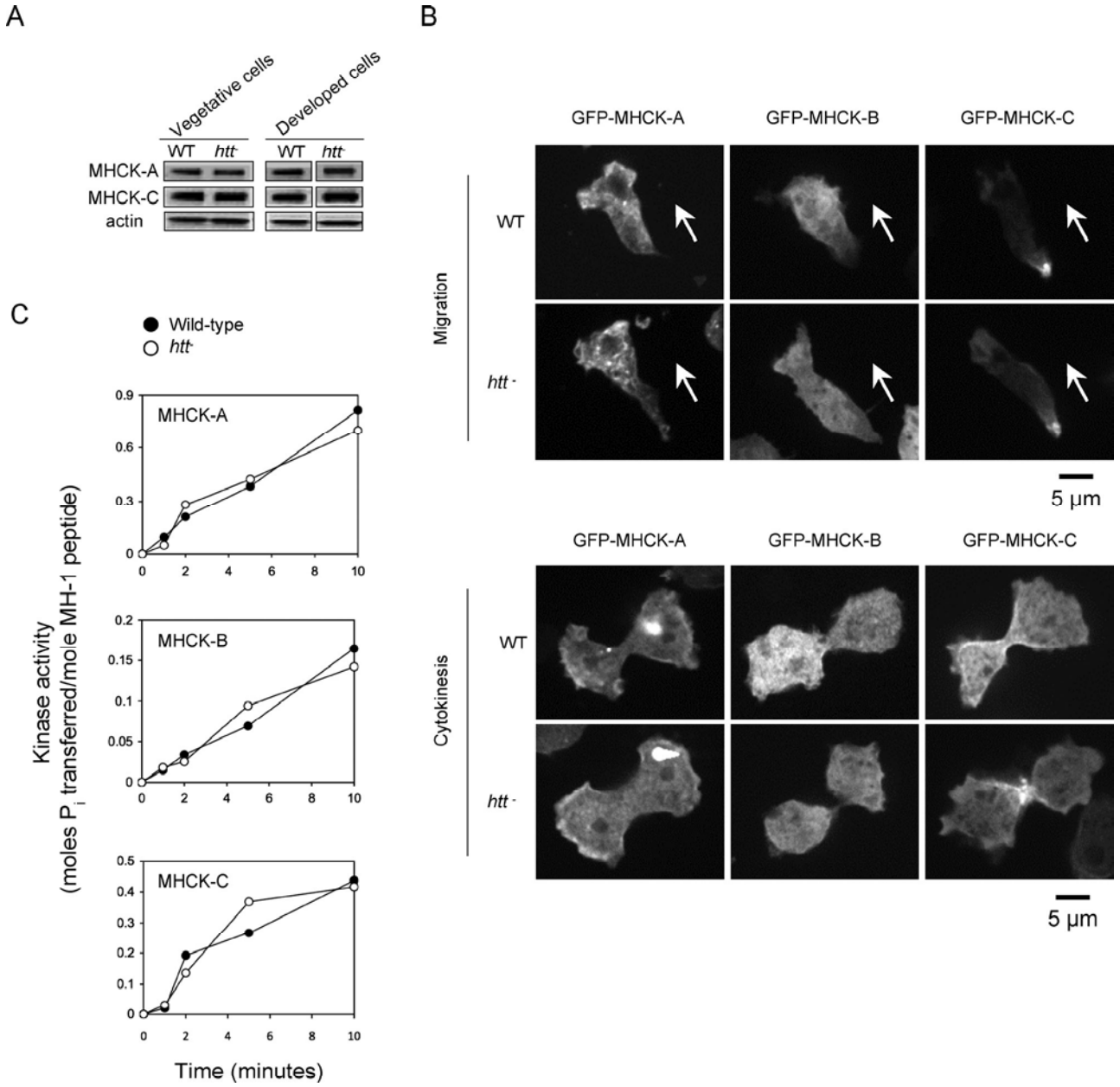

FIGURE 6: MHCKs are not affected in *htt*⁻ cells. (A) Abundance of MHCKs. Whole-cell lysates were analyzed by immunoblotting using the indicated antibodies. (B) Localization of GFP-MHCKs. We observed similar localization of MHCK-A, -B, and -C in wild-type and *htt*⁻ cells during migration and cytokinesis. During migration, MHCK-A and -C were located at the leading and trailing edge, respectively. We also observed punctate patterns, which might reflect aggregation of GFP fusion proteins. During cytokinesis, MHCK-A was located at the polar cortex, while MHCK-C was present at the cleavage furrow. MHCK-B appeared to be evenly distributed in the cytoplasm during migration and cytokinesis. (C) Activity of MHCKs. GFP-MHCKs were immunopurified using beads coupled to anti-GFP antibodies. Purified GFP-MHCKs were incubated with [γ-^{32}P]ATP and MH-1 peptides derived from myosin II (Steimle *et al.*, 2001a). Activity was determined by measuring incorporation of ^{32}P into MH-1 peptides.

We found that knockdown of Htt also reduced the activity of PP2A in HeLa cells, suggesting that the role of Htt in PP2A activity is evolutionarily conserved. Although the assembly of mammalian myosin II is also regulated by heavy-chain phosphorylation (Vicente-Manzanares *et al.*, 2009), it remains to be determined whether PP2A regulates myosin II during cytokinesis or chemotaxis in mammalian cells. Nonetheless, since the loss of normal function of Htt could contribute at least partially to the pathogenesis of Huntington's disease (Harjes and Wanker, 2003; Caviston and Holzbaur, 2009), it would be interesting to further investigate the phosphorylation status of PP2A substrates in this disease. In addition, a recent study has shown that a PP2A-B55α complex regulates mitotic exit, most likely by dephosphorylating Cdk1 substrates in human cells (Schmitz *et al.* 2010). RNAi knockdown of B55α, a regulatory subunit of this PP2A complex, delays spindle disassembly, chromosome decondensation, and Golgi assembly. These findings and our current study suggest that PP2A plays a key regulatory role in the mitotic phase.

Dictyostelium cells can divide on surfaces or in suspension culture. However, suspension growth is highly restrictive for cells with defects in the cytokinetic machinery. As a result, many cytokinetic

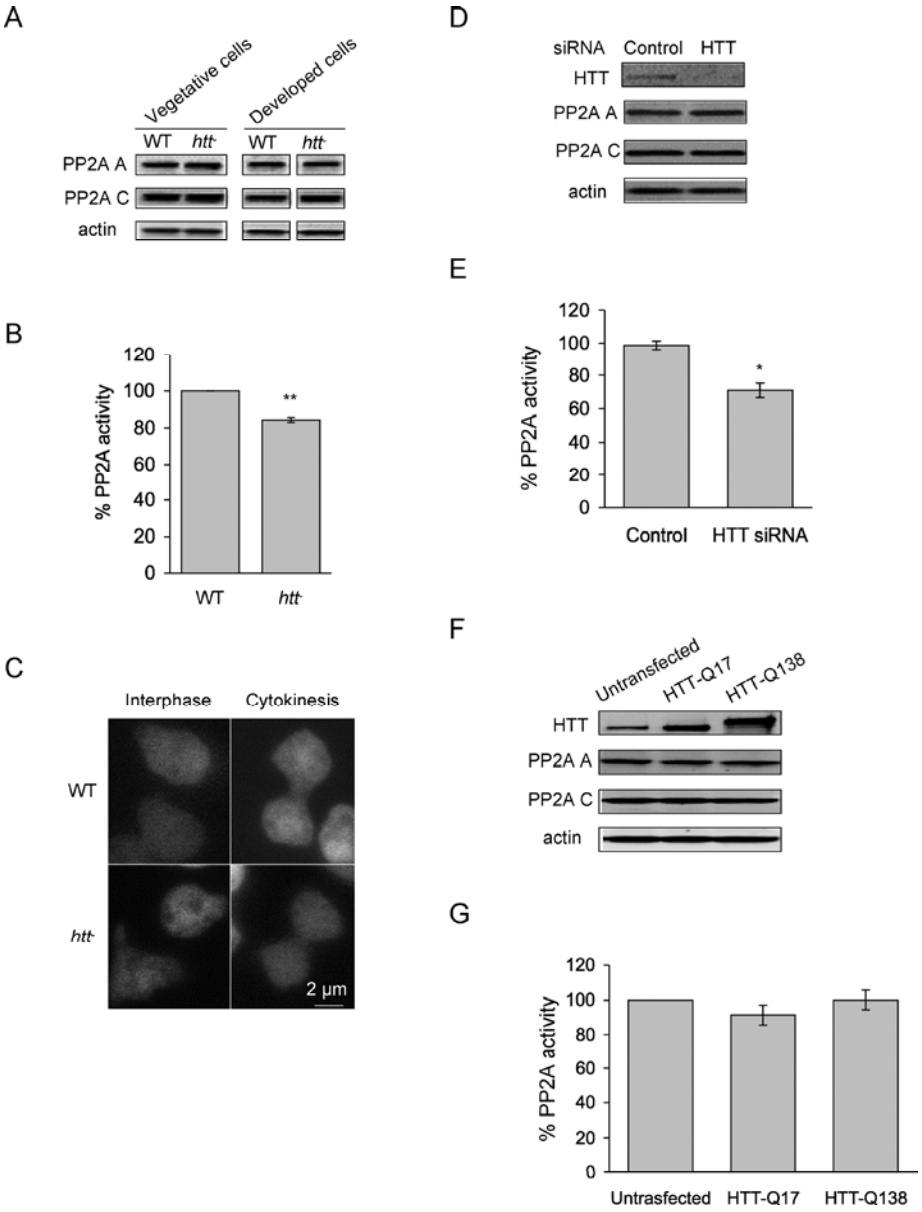

FIGURE 7: Htt is required for normal activity of PP2A in *Dictyostelium* and HeLa cells. (A) Quantity of PP2A subunits. Whole-cell lysates were analyzed by immunoblotting using the indicated antibodies. (B) Activity of PP2A was determined against threonine phosphopeptides (PP2A immunoprecipitation phosphatase assay kit, Millipore) and normalized to that of wild-type cells (n = 3). (C) Localization of PP2A A65-YFP. YFP (yellow fluorescent protein) was fused to the scaffolding subunit of PP2A and expressed in wild-type and *htt*⁻ cells. (D) Immunoblotting shows a decrease in HTT levels after siRNA depletion of HTT for 72 h. Whole-cell lysates were analyzed by immunoblotting using the indicated antibodies. (E) Activity of PP2A. PP2A activity was normalized to that of control siRNA (n = 3). (F) Overexpression of wild-type and mutant HTT. (G) Activity of PP2A. Activity was normalized to that of untransfected cells (n = 3).

mutants show quantitative defects under both growth conditions, but only fail at cytokinesis, becoming multinucleated only in suspension culture (Robinson, 2001; Uyeda and Nagasaki 2004). Therefore *htt*⁻ cells, like *mhcA* null cells, complete cytokinesis successfully on surfaces by drawing on adhesion properties but fail in suspension culture. However, *htt*⁻ cells formed GLCs, unlike *mhcA* null cells, which become enlarged and multinucleated. In addition, there are several *Dictyostelium* mutants that are defective in cytokinesis, none of which have been reported to form GLCs. Therefore Htt likely acts at an unidentified step during cytokinesis. Our study also suggests a novel role for myosin II in the completion of cytokinesis, in addition to its known role in the initiation and ingression of the cleavage furrow. The failure of myosin II maintenance at later stages of cytokinesis likely blocks abscission in *htt*⁻ cells, leading to the formation of GLCs.

MATERIALS AND METHODS

Cell culture, strains, and plasmids

All *Dictyostelium discoideum* cell lines were cultured in HL5 medium at 22°C. *htt*⁻ cells were generated by homologous recombination. The Htt targeting vector was constructed as follows: DNA fragments containing 5′ untranslated region (UTR) of *htt* was amplified from genomic DNA using primers 5′-TCAGCATCACCAATAGATACA-GAGG-3′ and 5′-ATATACTTTCTACATTTC-GATGGTC-3′. A DNA fragment containing the 3′UTR region was amplified using primers 5′-CATTGGATAGACAGAAATTCT-CACG-3′ and 5′- CTTTATTGAAATAAAAT-TCTGATGC-3′. These two DNA fragments and the blasticidin-S-resistance cassette from pLPBLPv2 (M. Landree, Johns Hopkins University, Baltimore, MD) were cloned into pBluescript (Stratagene, Agilent, Santa Clara, CA) to generate the targeting vector. The Htt targeting vector was linearized with *Not*I and introduced into growing AX2 cells by electroporation (Gaudet *et al.*, 2007). Transformants were selected in HL5 medium containing 5 µg/ml blasticidin (ICN Biomedicals, Costa Mesa, CA) on plastic dishes. After 5 d, cells were harvested and plated on SM agar plates with *Klebsiella aerogenes*. Randomly selected clones were screened for gene disruption by PCR and Southern blot analysis.

To clone the *Htt* gene, full-length *Htt* was amplified by PCR from three separate regions of the *Htt* gene of strain AX2 genomic DNA with primers based on the predicted DNA sequences of *Htt* in dictyBase (http://dictybase.org). To combine the three fragments, the internal restriction sites *Bam*HI, *Sca*I, *Nci*I, and *Xho*I were used. The full-length *Htt* gene was cloned into the *Bgl*II and *Xho*I site of GFP-PJK1 (Iijima and Devreotes, 2002). The resulting *htt*-GFP construct was confirmed by DNA sequencing.

The mycAhp and MHCK constructs have been described previously (Yumura *et al.*, 2005; Girard *et al.*, 2006).

Antibodies

We used antibodies against actin (C-11; Santa Cruz Biotechnology, Santa Cruz, CA), human Htt (#2773; Cell Signaling, Beverly, MA), PP2A-C subunit (HeLa cells: #2038; Cell Signaling; *Dictyostelium* cells: 1D6; Millipore, Billerica, MA), and PP2A-A subunit (HeLa cells: PP2A A subunit [81G5] rabbit monoclonal antibody #2041; Cell Signaling). Antibodies against *Dictyostelium* PP2A-A subunit

were described previously (Murphy and Egelhoff, 1999), as were antibodies against MHCK-A and -C (Yumura *et al.*, 2005).

Developmental assay

To assess developmental phenotypes, cells grown exponentially were washed twice in development buffer (DB: 10 mM phosphate buffer, 2 mM $MgSO_4$, 0.2 mM $CaCl_2$) and plated on 1% nonnutrient DB agar at a cell density of 5×10^5 cells/cm^2. To determine plaque size, cells were plated as individual clones with *K. aerogenes* on SM agar plates (10.0 g/l glucose, 10.0 g/l proteose peptone, 10.0 g/l yeast extract, 1.9 g/l KH_2PO_4, 1.0 g/l K_2HPO_4, 0.5 g/l $MgSO_4$, 15.0 g/l agar) and cultured at 22°C for 5 d.

Myosin II phosphorylation

Metabolic labeling with [^{32}P]orthophosphate was performed, as previously described (Berlot *et al.*, 1985). Approximately 8×10^7 aggregation-competent, caffeine-treated cells were incubated with [^{32}P]orthophosphate at 0.5 mCi/ml for 40 min. Cell suspensions containing ~5×10^7 cells were mixed with an equal volume of ice-cold 2× lysis buffer (200 mM NaF, 300 mM NaCl, 2% NP-40, 2 mM EDTA, 2 mM dithiothreitol [DTT], 2 mM ATP, 10 mM phosphate buffer, pH 6.8, protease inhibitor cocktail tablet, and phosphatase inhibitor cocktail tablet [Roche Applied Science, Indianapolis, IN]) and centrifuged for 20 min at 45,000 rpm in a TLA-55 (Beckman Coulter, Brea, CA). The supernatants were incubated with GFP antibody (Santa Cruz Biotechnology) and IgG-*Staphylococcus aureus* (Sigma-Aldrich, St. Louis, MO) for 3 h at 4°C. The samples were centrifuged and the pellets were washed three times with 1× lysis buffer. The pellets were resuspended in SDS–PAGE sample buffer and analyzed by immunoblotting using anti-GFP antibodies and autoradiography. For immunoblotting, proteins were visualized by fluorophores conjugated to secondary antibodies (ZyMax goat anti–rabbit IgG [H + L] Cy5 conjugate; Invitrogen, Carlsbad, CA) or an enhanced chemiluminescence detection system (Thermo Scientific, Lafayette, CO) and analyzed using a PharosFX Plus molecular imager (Bio-Rad, Hercules, CA), Quantity One (Bio-Rad), and Photoshop software (Adobe, San Jose, CA).

Measuring myosin II and actin in the cortex

Cells were developed and pretreated with caffeine, as previously described (Iijima and Devreotes, 2002). To obtain the Triton X-100–insoluble fraction, 5×10^6 cells were harvested and lysed in Triton X-100 buffer (1% Triton X-100, 10 mM KCl, 10 mM imidazole, 10 mM EGTA, 50 µg/ml NaN_3; Steimle *et al.*, 2001b). After mixing by vortex, samples were kept on ice for 10 min, and then further incubated at room temperature for 10 min. The samples were spun at $8000 \times g$ for 4 min. The pellet fractions were washed once with Triton X-100 buffer and then dissolved in 2× SDS–PAGE sample buffer. Proteins were resolved by SDS–PAGE and visualized by Coomassie Brilliant Blue staining. Myosin II and actin were quantified using Image J software (http://rsbweb.nih.gov/ij/download.html).

Chemotaxis assay

Cells grown in plastic dishes were washed twice with DB buffer, resuspended at 2×10^7 cells/ml, and shaken for 1 h before being induced to differentiate with 100 nM cAMP pulses at 6-min intervals for 4 h (Iijima and Devreotes, 2002). Chemotactic movements of cells to a micropipette containing cAMP were performed as previously described (Parent *et al.*, 1998). Differentiated cells were plated on a chambered coverglass (Lab-Tek; Nunc, Thermo Scientific) and allowed to adhere to the surface. A micropipette filled with 1 µM cAMP was positioned, and images of moving cells were recorded. Image J software was used to collect and process data. The motility speed was determined by measuring the position of the centroid every 30 s for a period of 10 min. The chemotaxis speed was calculated as the distance toward the micropipette divided by the elapsed time (10 min). The chemotaxis index was defined as the distance moved in the direction of the gradient divided by the total distance moved for 30-s intervals averaged during a period of 10 min. Roundness was determined by calculating the ratio of short axis (A_s) and long axis (A_l) of cells (A_s/A_l) (Loovers *et al.*, 2006).

Microscopy

Phase-contrast images of living cells in chemotaxis assays were obtained using an Olympus CKX41 inverted microscope equipped with a 10×/0.25 objective connected to a Scion CFW-1308M digital camera (Frederick, MD) that was operated with the Image J software. Differential interference contrast microscopy (DIC) and epifluorescence images of DAPI-stained cells were obtained on an Olympus IX81 inverted microscope equipped with a 40×/1.3 oil objective connected to an EM-CCD camera (C9100; Hamamatsu, Japan) and Slidebook software (3i, Denver, CO).

To observe cytokinesis on surfaces, cells were placed in Lab-Tek II chambers (Nunc, Thermo Scientific). To make the surface less adhesive, Lab-Tek II chambers were coated with Sigmacote (Sigma-Aldrich) according to the manufacturer's instructions. Once the cells had settled, the medium was replaced with DB-2-(*N*-morpholino)ethane sulfonic acid (DB-MES: 20 mM MES, pH 6.5, 2 mM $MgSO_4$, 0.2 mM $CaCl_2$). All data were analyzed with Image J software.

To observe GFP-myosin II, an Olympus IX81 inverted microscope equipped with a 40×/1.3 oil objective connected to an EM-CCD camera (C9100; Hamamatsu, Japan) and Slidebook software (3i) was used. For quantification of GFP-myosin II distribution, the fluorescent signal intensities of the cleavage furrow (Ic) and the polar cytoplasm (Ip) were measured and the Ic/Ip ratio was calculated (Robinson and Spudich, 2000).

MHCK activity assay

Wild-type and *htt*$^-$ cells were transfected with plasmids GFP-fused to MHCKs and transformants were selected in the presence of 10 µg/ml G418. The GFP fusion proteins were immunoprecipitated from 10^7 cells using 20 µl of packed GFP-Trap beads (Allele Biotech, San Diego, CA) following the manufacturer's protocol, except that 0.5% Triton X-100 was used in place of 0.5% NP40. For quantification, purified kinases were subjected to SDS–PAGE with a series of known amounts of bovine serum albumin (BSA) on the same gel. After Coomassie Brilliant Blue staining, the protein bands were quantified by scanning densitometry, and the concentration of each purified fusion protein was determined by comparing the densitometry values for the purified kinases with those of the BSA standards in the same gel. Immunoprecipitated MHCK-A, -B, and -C (100 nM) were assayed for kinase activity toward MH-1 peptide substrate (50 µM) as has been described in detail previously (Steimle *et al.*, 2001a; Egelhoff *et al.*, 2005). Briefly, all kinase assays were performed at 25°C in 10 mM TES, pH 7.0, 2 mM $MgCl_2$, 0.5 mM DTT, and 0.5 mM [γ-^{32}P]ATP (250–400 Ci/mol). The peptide sequence of the MH-1 substrate (RKKFGESEKTKTKEFL-amide) was synthesized by New England Peptide (Gardner, MA) and contains the sequence corresponding to the mapped MHCK-A target site in the myosin II tail at residue 2029 (underlined in peptide sequence above). Kinase reactions

were stopped by blotting a fraction of the reaction mixture onto P-81 filter paper (Whatman, Piscataway, NJ) and then processing the filter for quantification via scintillation counting.

PP2A activity assay

PP2A activity was measured by release of phosphates from phosphopeptides (K-R-pT-I-R-R) using a Malachite Green assay (PP2A immunoprecipitation phosphatase assay kit; Millipore) as previously described (Lee *et al.*, 2008). The activity was normalized to cell numbers.

Transfection of HeLa cells

HeLa cells (2×10^5 cells/well) were transfected in six-well plates with 20 nM Silencer Select Pre-designed Htt siRNA (siRNA ID: S6490; Ambion, Austin, TX) using 4 µl siPORT NeoFX (Ambion) per well. The medium was replaced with fresh culture medium (DMEM supplemented with fetal bovine serum [FBS]) at 24 h after transfection. Nontargeting siRNA (AM4635; Ambion) was used as a negative control. Lipofectamine 2000 (Invitrogen) was used to transfect HeLa cells with wild-type Htt (pTre2Hyg:3xFLAG:HD 17Q full length) and mutant Htt (pTre2Hyg:3xFLAG:HD138Q full length; Rubinsztein and Carmichael, 2003) plasmids according to the manufacturer's instructions. Cells were lysed at 72 h after transfection to measure the PP2A activity.

Statistical analysis

All values are means ± SEM. Results were statistically analyzed using Student's *t* test (*, $p < 0.05$; **, $p < 0.01$).

ACKNOWLEDGMENTS

We are grateful to David C. Rubinsztein (Department of Medical Genetics, Cambridge Institute for Medical Research, Cambridge, UK) for kindly providing Htt plasmids. We thank members of the Iijima and Sesaki laboratories for helpful discussion. This work was supported by American Heart Association grant 0765345U and National Institutes of Health grant GM-084015 to M.I.; National Institutes of Health grant GM089853, American Heart Association grant 0730247N, and Muscular Dystrophy grant 69361 to H.S.; National Institutes of Health grant GM066817 to D.N.R.; National Institutes of Health grant GM50009 to T.T.E.; and National Institutes of Health grant 2R15GM066789 to P.A.S.

REFERENCES

Annesley SJ, Fisher PR (2009). *Dictyostelium discoideum*—a model for many reasons. Mol Cell Biochem 329, 73–91.

Berlot CH, Spudich JA, Devreotes PN (1985). Chemoattractant-elicited increases in myosin phosphorylation in dictyostelium. Cell 43, 307–314.

Bosgraaf L, van Haastert PJ (2002). A model for cGMP signal transduction in Dictyostelium in perspective of 25 years of cGMP research. J Muscle Res Cell Motil 23, 781–791.

Bosgraaf L, van Haastert PJ (2006). The regulation of myosin II in Dictyostelium. Eur J Cell Biol 85, 969–979.

Caviston JP, Holzbaur EL (2009). Huntingtin as an essential integrator of intracellular vesicular trafficking. Trends Cell Biol 19, 147–155.

De la Roche MA, Smith JL, Betapudi V, Egelhoff TT, Cote GP (2002). Signaling pathways regulating Dictyostelium myosin II. J Muscle Res Cell Motil 23, 703–718.

Egelhoff TT, Croft D, Steimle PA (2005). Actin activation of myosin heavy chain kinase A in *Dictyostelium*: a biochemical mechanism for the spatial regulation of myosin II filament disassembly. J Biol Chem 280, 2879–2887.

Funamoto S, Meili R, Lee S, Parry L, Firtel RA (2002). Spatial and temporal regulation of 3-phosphoinositides by PI 3-kinase and PTEN mediates chemotaxis. Cell 109, 611–623.

Gaudet P, Pilcher KE, Fey P, Chisholm RL (2007). Transformation of *Dictyostelium* discoideum with plasmid DNA. Nat Protoc 2, 1317–1324.

Gil JM, Rego AC (2008). Mechanisms of neurodegeneration in Huntington's disease. Eur J Neurosci 27, 2803–2820.

Girard KD, Kuo SC, Robinson DN (2006). *Dictyostelium* myosin II mechanochemistry promotes active behavior of the cortex on long time scales. Proc Natl Acad Sci USA 103, 2103–2108.

Harjes P, Wanker EE (2003). The hunt for huntingtin function: interaction partners tell many different stories. Trends Biochem Sci 28, 425–433.

Iijima M, Devreotes P (2002). Tumor suppressor PTEN mediates sensing of chemoattractant gradients. Cell 109, 599–610.

Iijima M, Huang YE, Luo HR, Vazquez F, Devreotes PN (2004). Novel mechanism of PTEN regulation by its phosphatidylinositol 4,5-bisphosphate binding motif is critical for chemotaxis. J Biol Chem 279, 16606–16613.

Jeon TJ, Lee DJ, Merlot S, Weeks G, Firtel RA (2007). Rap1 controls cell adhesion and cell motility through the regulation of myosin II. J Cell Biol 176, 1021–1033.

Lee NS, Veeranki S, Kim B, Kim L (2008). The function of PP2A/B56 in nonmetazoan multicellular development. Differentiation 76, 1104–1110.

Lee S, Shen Z, Robinson DN, Briggs S, Firtel RA (2010). Involvement of the cytoskeleton in controlling leading-edge function during chemotaxis. Mol Biol Cell 21, 1810–1824.

Levi S, Polyakov MV, Egelhoff TT (2002). Myosin II dynamics in *Dictyostelium*: determinants for filament assembly and translocation to the cell cortex during chemoattractant responses. Cell Motil Cytoskeleton 53, 177–188.

Loovers HM, Postma M, Keizer-Gunnink I, Huang YE, Devreotes PN, van Haastert PJ (2006). Distinct roles of PI(3,4,5)P3 during chemoattractant signaling in *Dictyostelium*: a quantitative in vivo analysis by inhibition of PI3-kinase. Mol Biol Cell 17, 1503–1513.

MacDonald ME, Gines S, Gusella JF, Wheeler VC (2003). Huntington's disease. Neuromol Med 4, 7–20.

Murphy MB, Egelhoff TT (1999). Biochemical characterization of a *Dictyostelium* myosin II heavy-chain phosphatase that promotes filament assembly. Eur J Biochem 264, 582–590.

Nagasaki A, Itoh G, Yumura S, Uyeda TQ (2002). Novel myosin heavy chain kinase involved in disassembly of myosin II filaments and efficient cleavage in mitotic *Dictyostelium* cells. Mol Biol Cell 13, 4333–4342.

Parent CA, Blacklock BJ, Froehlich WM, Murphy DB, Devreotes PN (1998). G protein signaling events are activated at the leading edge of chemotactic cells. Cell 95, 81–91.

Pollard TD (2010). Mechanics of cytokinesis in eukaryotes. Curr Opin Cell Biol 22, 50–56.

Rai V, Egelhoff TT (2011). Role of B regulatory subunits of protein phosphatase type 2A in myosin II assembly control in *Dictyostelium discoideum*. Eukaryot Cell. 10, 604–610.

Reichl EM, Ren Y, Morphew MK, Delannoy M, Effler JC, Girard KD, Divi S, Iglesias PA, Kuo SC, Robinson DN (2008). Interactions between myosin and actin crosslinkers control cytokinesis contractility dynamics and mechanics. Curr Biol 18, 471–480.

Robinson DN (2001). Cell division: biochemically controlled mechanics. Curr Biol 11, R737–R740.

Robinson DN, Girard KD, Octtaviani E, Reichl EM (2002). *Dictyostelium* cytokinesis: from molecules to mechanics. J Muscle Res Cell Motil 23, 719–727.

Robinson DN, Spudich JA (2000). Dynacortin, a genetic link between equatorial contractility and global shape control discovered by library complementation of a *Dictyostelium discoideum* cytokinesis mutant. J Cell Biol 150, 823–838.

Robinson DN, Spudich JA (2004). Mechanics and regulation of cytokinesis. Curr Opin Cell Biol 16, 182–188.

Ross CA (2002). Polyglutamine pathogenesis: emergence of unifying mechanisms for Huntington's disease and related disorders. Neuron 35, 819–822.

Ross CA (2004). Huntington's disease: new paths to pathogenesis. Cell 118, 4–7.

Rubinsztein DC, Carmichael J (2003). Huntington's disease: molecular basis of neurodegeneration. Expert Rev Mol Med 5, 1–21.

Schmitz MH *et al.* (2010). Live-cell imaging RNAi screen identifies PP2A-B55α and importin-β1 as key mitotic exit regulators in human cells. Nat Cell Biol 12, 886–893.

Steimle PA, Naismith T, Licate L, Egelhoff TT (2001a). WD repeat domains target Dictyostelium myosin heavy chain kinases by binding directly to myosin filaments. J Biol Chem 276, 6853–6860.

Steimle PA, Yumura S, Cote GP, Medley QG, Polyakov MV, Leppert B, Egelhoff TT (2001b). Recruitment of a myosin heavy chain kinase to actin-rich protrusions in *Dictyostelium*. Curr Biol 11, 708–713.
Swaney KF, Huang CH, Devreotes PN (2010). Eukaryotic chemotaxis: a network of signaling pathways controls motility, directional sensing, and polarity. Annu Rev Biophys 39, 265–289.
Uyeda TQ, Nagasaki A (2004). Variations on a theme: the many modes of cytokinesis. Curr Opin Cell Biol 16, 55–60.
Vicente-Manzanares M, Ma X, Adelstein RS, Horwitz AR (2009). Non-muscle myosin II takes centre stage in cell adhesion and migration. Nat Rev Mol Cell Biol 10, 778–790.
Williams RS, Boeckeler K, Graf R, Muller-Taubenberger A, Li Z, Isberg RR, Wessels D, Soll DR, Alexander H, Alexander S (2006). Towards a molecular understanding of human diseases using *Dictyostelium discoideum*. Trends Mol Med 12, 415–424.
Yumura S, Fukui Y (1985). Reversible cyclic AMP-dependent change in distribution of myosin thick filaments in *Dictyostelium*. Nature 314, 194–196.
Yumura S, Uyeda TQ (2003). Myosins and cell dynamics in cellular slime molds. Int Rev Cytol 224, 173–225.
Yumura S, Yoshida M, Betapudi V, Licate LS, Iwadate Y, Nagasaki A, Uyeda TQ, Egelhoff TT (2005). Multiple myosin II heavy chain kinases: roles in filament assembly control and proper cytokinesis in *Dictyostelium*. Mol Biol Cell 16, 4256–4266.

A

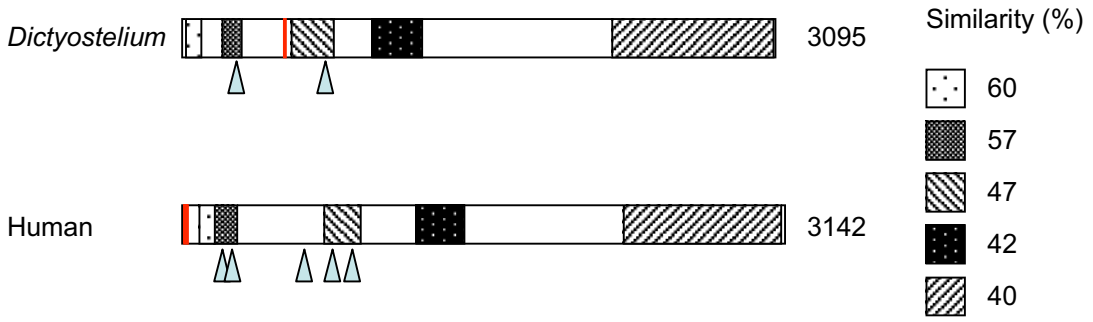

B

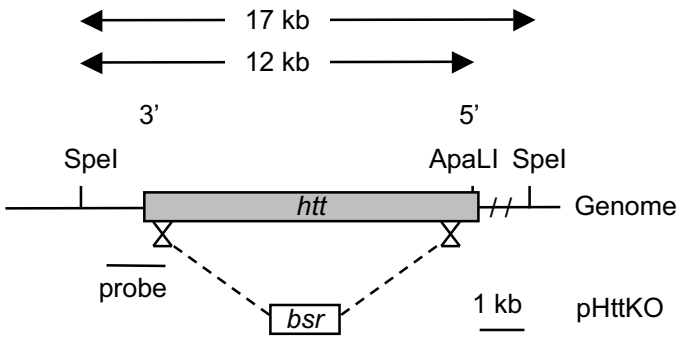

C

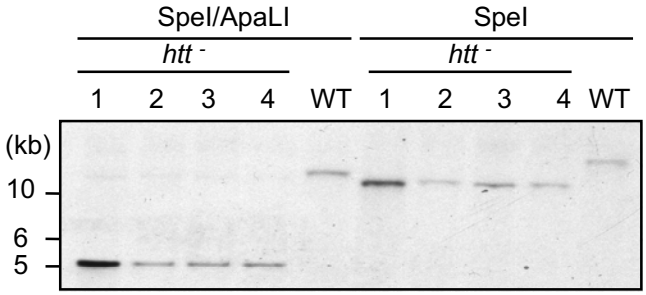

Wang et al. Figure S1

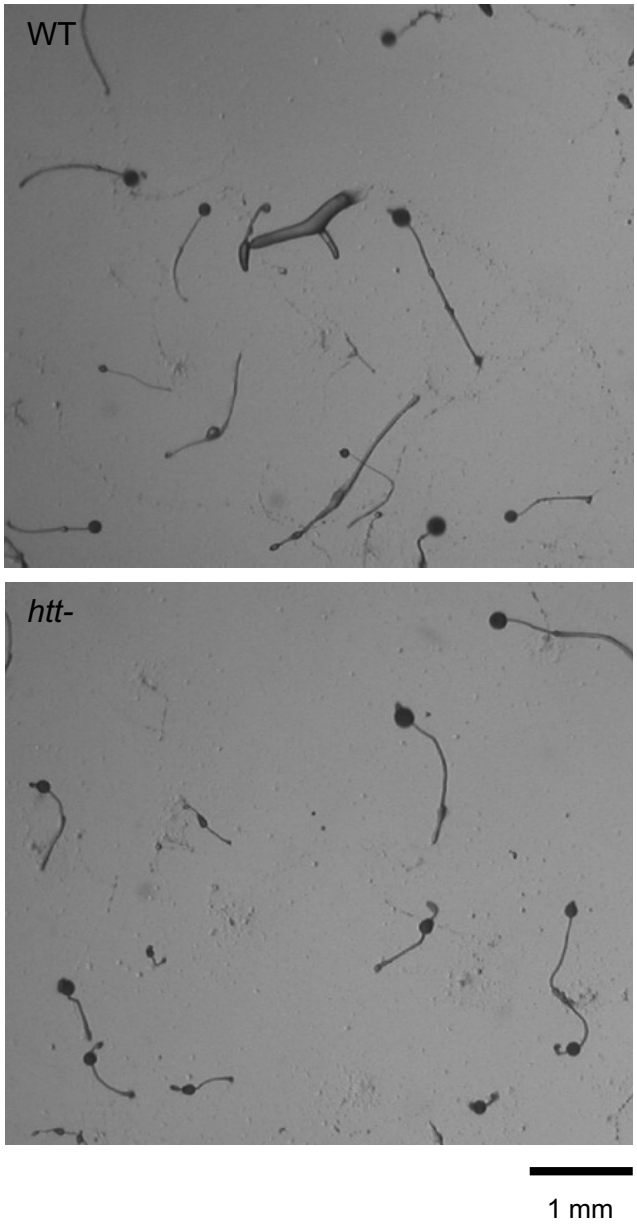

Fruiting bodies/cm^2

Wildtype	: 33.1 ± 2.4 (n = 4)
htt-	: 32.6 ± 1.2 (n = 8)

Wang et al. Figure S2

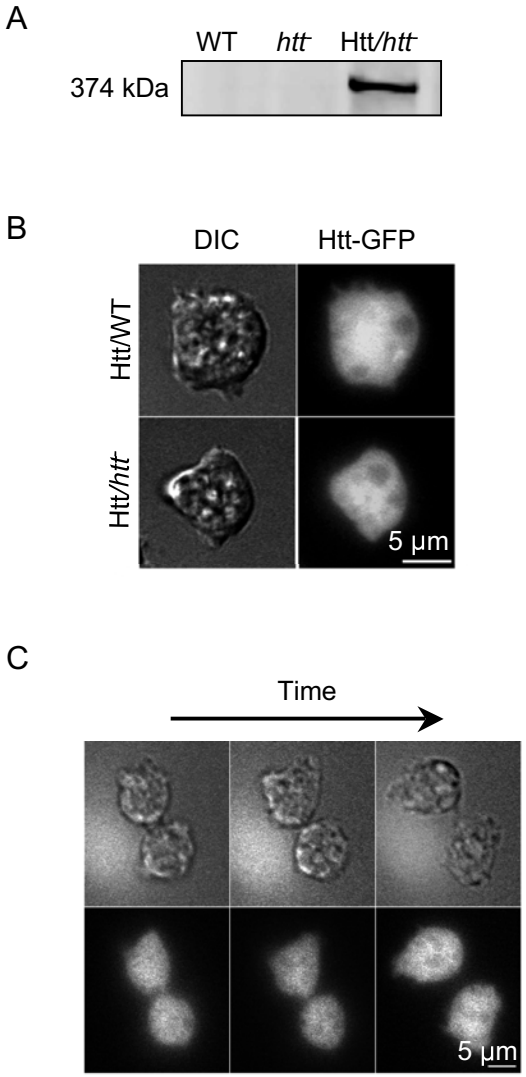

Wang et al. Figure S3

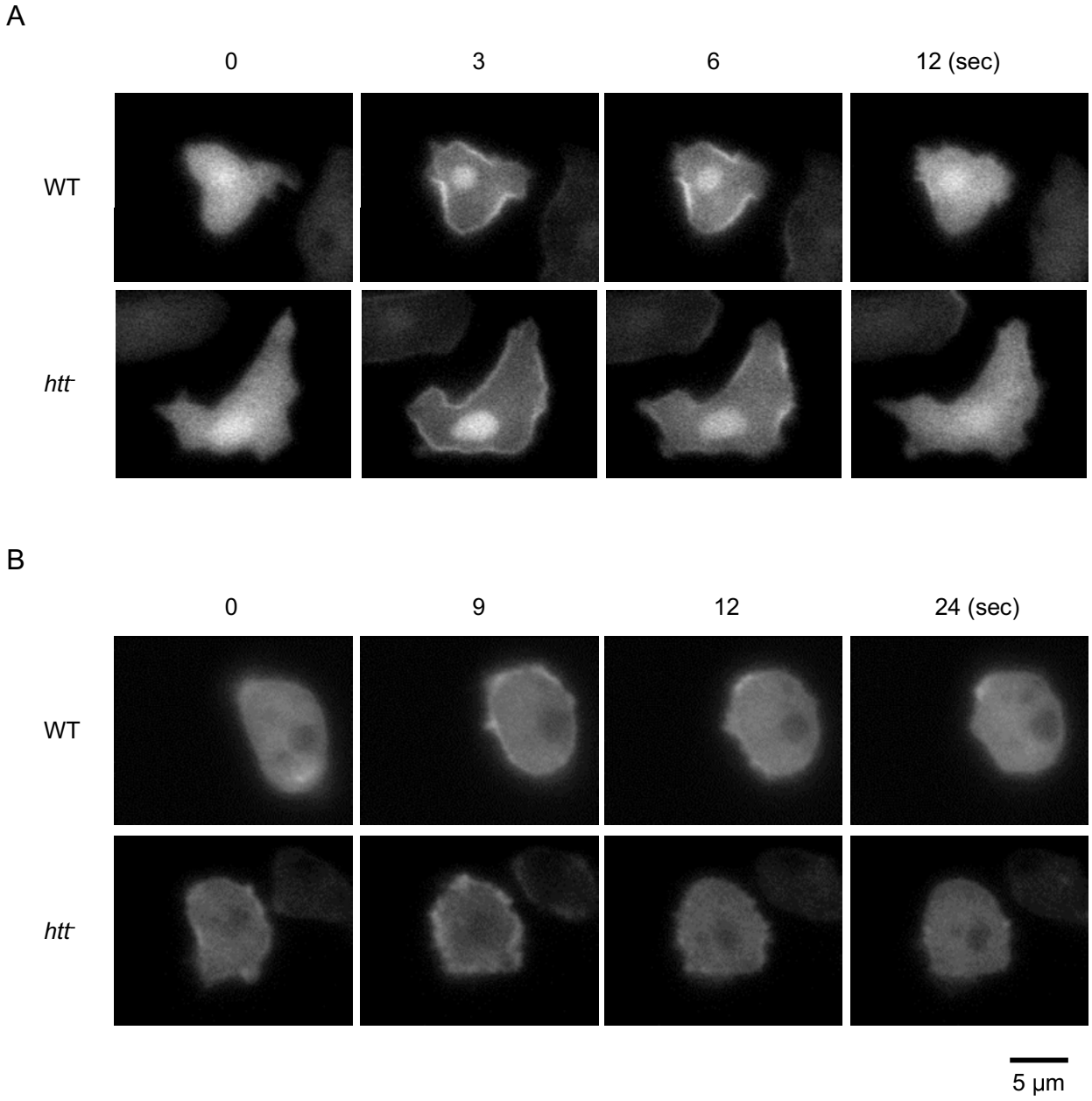

Wang et al. Figure S4

MHCK-A overexpression

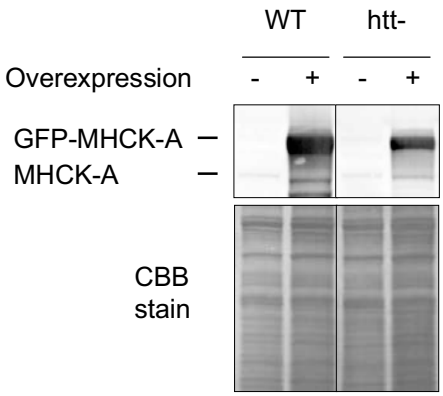

MHCK-C overexpression

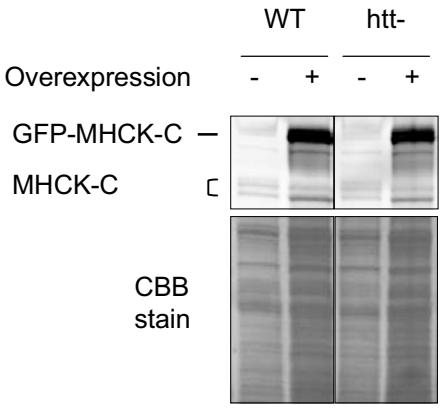

Wang et al. Figure S5

A) No overexpression

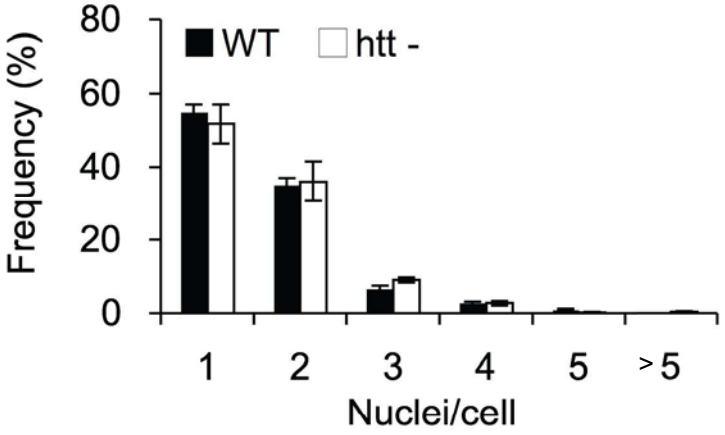

B) GFP-MHCK-A overexpression

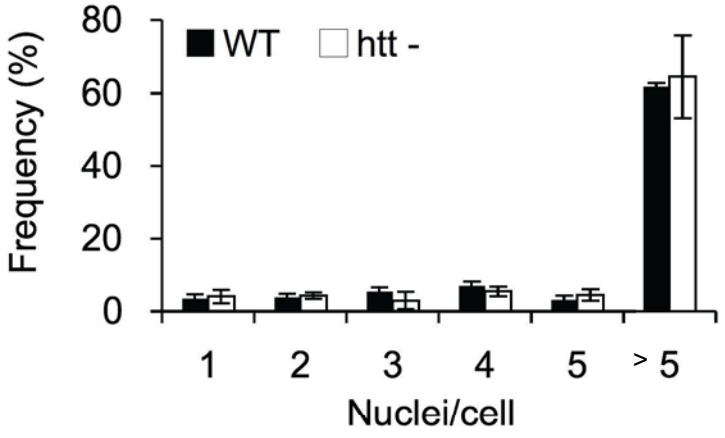

C) GFP-MHCK-C-overexpression

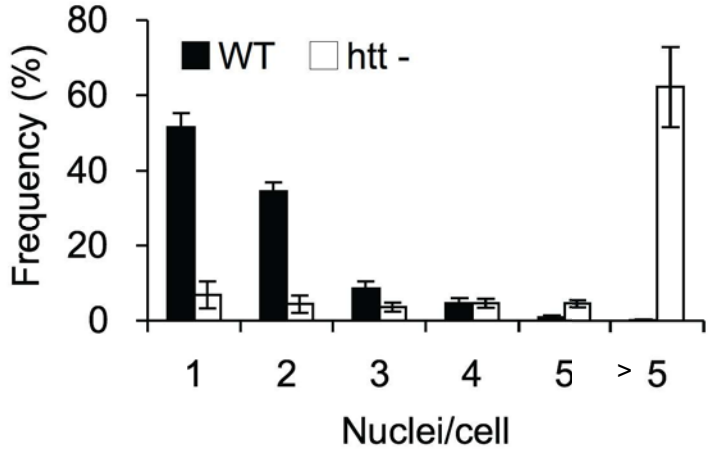

Wang et al. Figure S6

(A) GFP-MHCK A

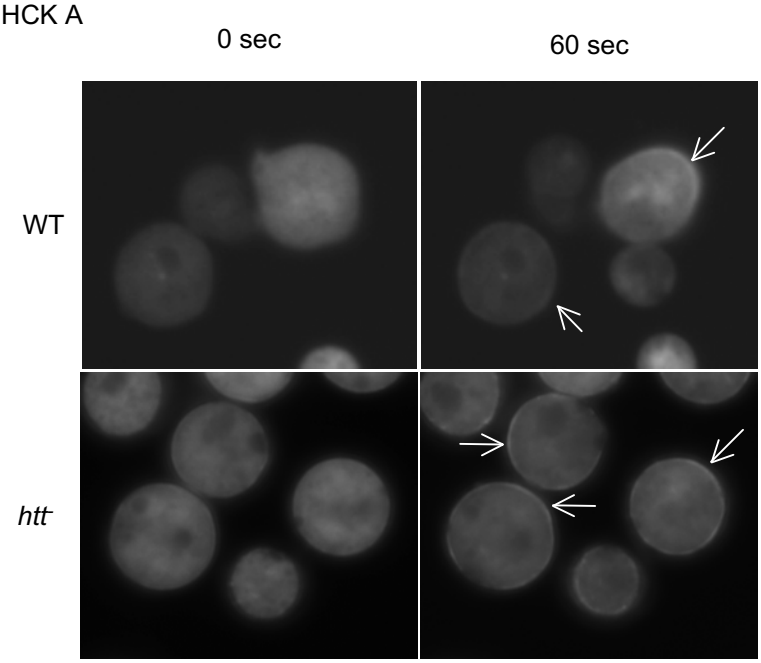

(B) GFP-MHCK C

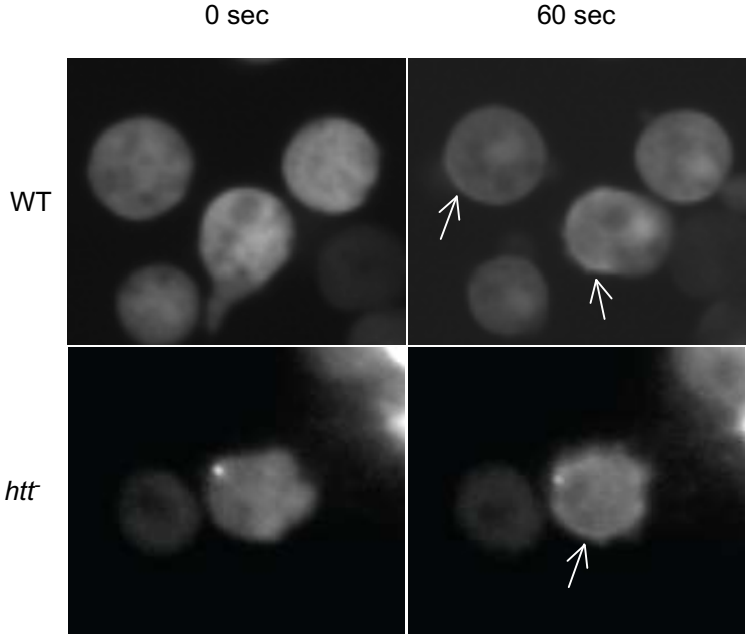

Wang et al. Figure S7

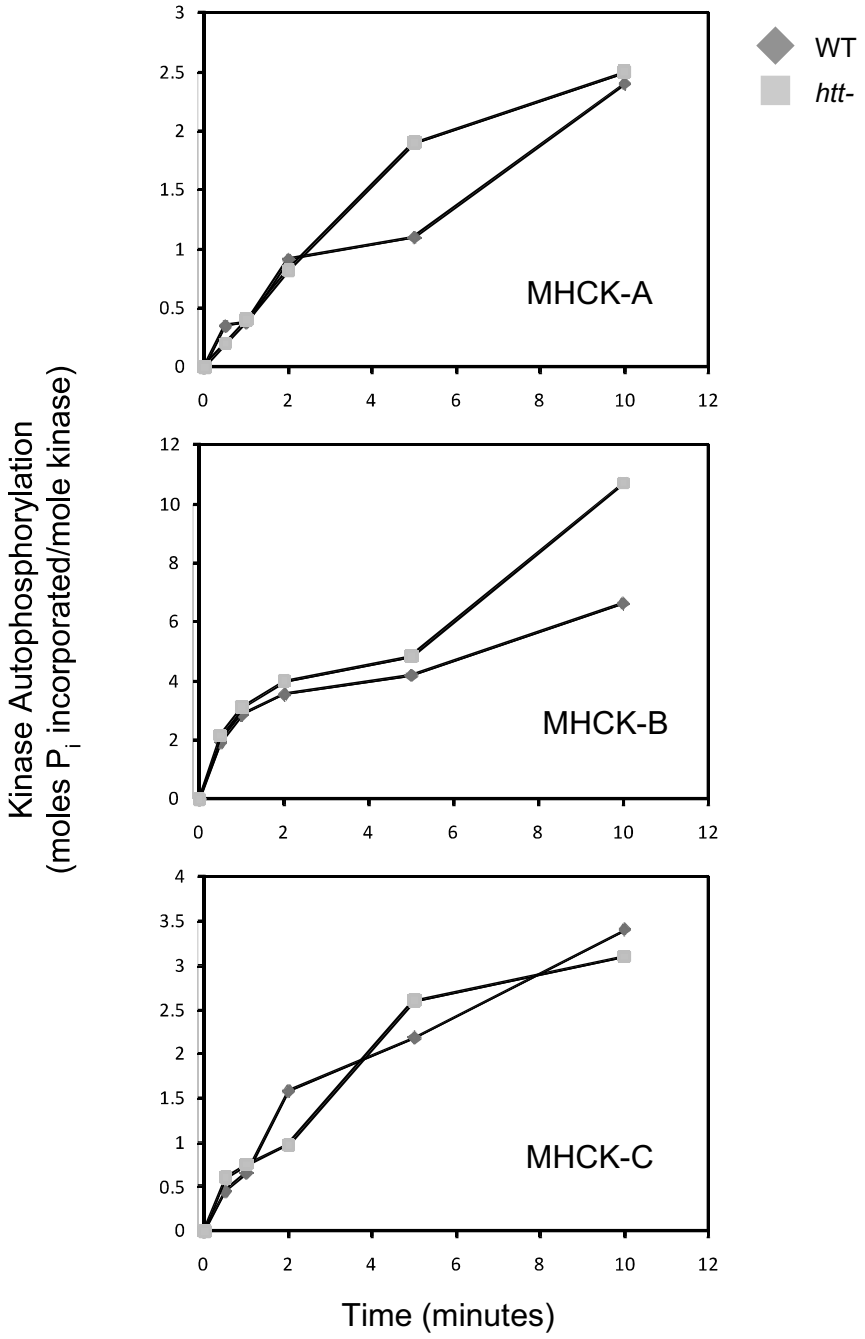

Wang et al. Figure S8

Table S1. PP2A regulatory subunits

Family	***H. sapiens***	***D. discoideum***
PTP/PR53	PPP2R4	DDB_G0270036/ppp2r4
		DDB_G0279655
B/PR55	PPP2R2A	DDB_G0283905/phr2aB
	PPP2R2B	DDB_G0293386
	PPP2R2C	
	PPP2R2D	
B'/PR61	PPP2R5A	DDB_G0280469/psrA
	PPP2R5B	
	PPP2R5C	
	PPP2R5D	
	PPP2R5E	
B''/PR72	PPP2R3A	DDB_G0279813
	PPP2R3B	
	PPP2R3C	
B'''/PR110	STRN	
	STRN3	